Published in final edited form as:
Hum Mol Genet. 2014 April 01; 23(7): 1842–1855. doi:10.1093/hmg/ddt577.

The transgenic expression of LARGE exacerbates the muscle phenotype of dystroglycanopathy mice

Charlotte Whitmore[1,2,#], **Marta Fernandez-Fuente**[1,#], **Helen Booler**[1], **Callum Parr**[1], **Manoli Kavishwar**[1], **Attia Ashraf**[3], **Erica Lacey**[1], **Jihee Kim**[1], **Rebecca Terry**[1], **Mark R. Ackroyd**[1], **Kim E. Wells**[1], **Francesco Muntoni**[3], **Dominic J. Wells**[1], and **Susan C. Brown**[*,1]

[1]Comparative Biomedical Sciences, Royal Veterinary College, University of London

[2]Division of Brain Sciences, Department of Medicine, Imperial College London

[3]Dubowitz Neuromuscular Unit, Institute of Child Health, UCL

Abstract

Mutations in fukutin related protein (FKRP) underlie a group of muscular dystrophies associated with the hypoglycosylation of α-dystroglycan (α-DG), a proportion of which show central nervous system involvement. Our original FKRP knock down mouse ($FKRP^{KD}$) replicated many of the characteristics seen in patients at the severe end of the dystroglycanopathy spectrum but died perinatally precluding its full phenotyping and use in testing potential therapies. We have now overcome this by crossing $FKRP^{KD}$ mice with those expressing Cre recombinase under the Sox1 promoter. Due to our original targeting strategy this has resulted in the restoration of Fkrp levels in the central nervous system but not the muscle, thereby generating a new model ($FKRP_{MD}$) which develops a progressive muscular dystrophy resembling what is observed in limb girdle muscular dystrophy. Like-acetylglucosaminyltransferase (LARGE) is a bifunctional glycosyltransferase previously shown to hyperglycosylate α-dystroglycan. In order to investigate the therapeutic potential of LARGE up-regulation we have now crossed the $FKRP_{MD}$ line with one overexpressing LARGE and show that, contrary to expectation, this results in a worsening of the muscle pathology implying that any future strategies based upon LARGE up-regulation require careful management.

Keywords

dystroglycan; fukutin related protein; LARGE; muscular dystrophy

Introduction

Dystroglycan (DG) forms the central component of the dystrophin associated protein complex and has been attributed with a primary role in the deposition, organisation and turnover of basement membranes (1–7). It is composed of two subunits, both of which are

Address for correspondence: S.C.Brown (020 7468 1212, scbrown@rvc.ac.uk) - Comparative Biomedical Sciences, Royal Veterinary College, London, United Kingdom NW1 0TU.

[#]The authors wish it to be known that, in their opinion, the first two authors should be regarded as joint First Authors.

Conflict of Interest: None declared.

Europe PMC Funders Author Manuscripts

encoded by the *DAG1* gene: β-DG, a transmembrane protein and α-DG, a highly glycosylated peripheral membrane protein (1). The primary sequence of α-DG predicts a molecular mass of 72kDa: however, due to extensive post-translational glycosylation the final molecular weight is around 156kDa in skeletal muscle (8). The O-linked glycan chains of the central mucin domain of α-DG mediate binding to basement membrane ligands including laminin (9), perlecan (10) agrin (11–13), neurexin in the brain (14), pikachurin in the eye (15) and Slit (16) by interaction with the laminin LG (laminin globular) domains (17,18) and their loss from the central mucin domain of α-DG is considered to be central to the pathogenesis of a subgroup of congenital muscular dystrophies (CMDs), the dystroglycanopathies (7,19–21).

To date at least 15 genes have been implicated in the glycosylation and/or processing of αDG, which now include *POMT1 (PROTEIN O-MANNOSYL-TRANSFERASE 1)* (22), *POMT2 (PROTEIN O-MANNOSYL-TRANSFERASE 2)* (23), *POMGNT1 (PROTEIN O-MANNOSE BETA-1,2-N-ACETYLGLUCOSAMINYLTRANSFERASE)* (24), *LARGE* (25–27), *FKT* (*FUKUTIN)* (28), *FKRP* (29,30), *DPM2 (DOLICHYL-PHOSPHATE MANNOSYLTRANSFERASE POLYPEPTIDE 2), DPM3 (DOLICHYL-PHOSPHATE MANNOSYLTRANSFERASE POLYPEPTIDE 3*) (31), *ISPD (ISOPRENOID SYNTHASE DOMAIN CONTAINING)* (32,33), *GTDC2 (GLYCOSYLTRANSFERASE-LIKE DOMAIN CONTAINING 2)* (34), *TMEM5 (TRANSMEMBRANE PROTEIN 5)* (35), *B3GNT1 (BETA-1,3-N-ACETYLGLUCOSAMINYLTRANSFERASE 1)* (36), *DOLK (DOLICHOL KINASE)* (37), *SGK196 (SUGEN KINASE 196)* (38) and *GMPPB (GDP-MANNOSE PYROPHOSPHORYLASE B)* (39). Mutations in these genes are often associated with a wide clinical spectrum of phenotypes, including severe CMD and structural brain defects as exemplified by Walker Warburg syndrome (WWS) OMIM 236670, Muscle Eye Brain disease (MEB) OMIM 253280, Fukuyama CMD (FCMD) OMIM 253800, and congenital muscular dystrophy type 1D (MDC1D) OMIM 608840). Whilst the precise pathway in which these proteins function is unclear, recent work suggests that SGK196 is a glycosylation specific O-mannose kinase and that FKRP, FKTN, TMEM5, B3GNT1 and LARGE all contribute to the generation of an extracellular matrix binding moiety on the resulting phosphorylated core M3 glycan (38). The loss of matrix binding is associated with a profound reduction in the binding of either IIH6 and/or VIA4-1 antibodies to α-dystroglycan (40). In addition a deficiency of Dol-P-Man synthase subunit DPM2 and DPM3 indicates a possible link between the congenital disorders of glycosylation and the dystroglycanopathies. However, it is mutations in FKRP that underlie LGMD2I, which is one of the most frequent autosomal recessive forms of LGMD (Limb girdle muscular dystrophy) in the UK, reported to make up 19.1% of the total LGMD group, with a prevalence of 0.43/100 000.

We previously generated a mouse model for FKRP related disease by inducing a knock-down in Fkrp expression via the insertion of a floxed Neomycin cassette into intron 2 of the mouse *Fkrp* gene ($FKRP^{KD}$). This resulted in perinatal lethality due to central nervous system involvement and whilst this model has proved useful in studies of disease pathogenesis, it is limited in regard to its potential for evaluating potential therapies aimed at restoring muscle function. In order to overcome this we have now crossed the $FKRP^{KD}$ line of mice with one expressing *Cre recombinase* under the control of the Sox1 (Sex

determining region Y-box 1) promoter, and show here that this strategy successfully restored Fkrp activity in the brain but not muscle. This new line, henceforth referred to as $FKRP_{MD}$, lives a normal lifespan and begins to show muscle damage at around 6 weeks of age and develops a progressive muscular dystrophy by 12 weeks, thereby representing a new mouse model of the less severe end of the dystroglycanopathy spectrum.

Whilst there have been two recent reports of the successful restoration of functional glycosylation and amelioration of the muscle pathology by AAV (Adeno-Associated Virus) vectors carrying either FKRP (41) or fukutin (42), one of the most promising forms of therapy proposed in recent years for the dystroglycanopathies is the up-regulation of LARGE; a bifunctional glycosyltransferase that alternately transfers xylose and glucuronic acid to generate a heteropolysaccharide that confers α-dystroglycan with its ligand binding properties (43). This is based on observations showing that LARGE is able to restore α-dystroglycan glycosylation and functional laminin binding to cells taken from patients with congenital muscular dystrophy (FCMD, MEB and WWS), seemingly irrespective of the gene involved (44). Whilst this response may be dependent on the availability of O-mannosyl phosphate acceptor sites (32), this strategy is still considered as being potentially useful for a wide range of patients. We have previously shown that in mice, over-expression of LARGE on a wild type background induces no overt pathology and is only associated with a minor loss of force in response to eccentric exercise in older mice, supporting the idea that increasing levels of this glycosyltransferase may represent an important therapeutic approach (45). However, it remains crucial to test such a strategy on a disease background and in order to do this we crossed our newly generated $FKRP_{MD}$ mouse line with one of the original *LARGE* overexpressing lines (45). Somewhat surprisingly we report that this fails to ameliorate the phenotype and in a proportion of mice leads to a worsening of the disease process despite a marked increase in dystroglycan glycosylation implying that any future strategies based upon LARGE up-regulation require careful management.

Results

Restoration of Fkrp levels in the central nervous system prevents the perinatal lethality of $FKRP^{KD}$ mice

$FKRP^{KD}$ mice have a significant reduction in *Fkrp* expression in the muscle and brain, compared to wild type mice, which we attributed to the insertion of the floxed Neomycin cassette into intron 2 (46). Since we believed that central nervous system involvement was responsible for the perinatal mortality, we set out to restore *Fkrp* expression in the central nervous system by crossing the $FKRP^{KD}$ line with one expressing Cre recombinase under the Sox1 promoter. $FKRP^{KD}$ mice expressing the Sox1 Cre transgene are henceforth referred to as $FKRP_{MD}$. This cross should delete the neomycin cassette from exon 2 in neurectoderm derived tissues. Since defects in the pial basement membrane due to a loss of α-dystroglycan are thought to be central to the brain phenotype of $FKRP^{KD}$ mice (46,47) we examined paraffin wax embedded coronal sections of the cortex of newborn mice. These sections showed a clear disruption of cortical architecture in the $FKRP^{KD}$ (Figure 1B) but no overt abnormalities in the $FKRP_{MD}$ mice, the latter of which were comparable to wild type (Figure 1A and C). IIH6 immunolabelling at the pial basement membrane of the $FKRP_{MD}$

was comparable to that of WT (Figure 1A and C) but not the $FKRP^{KD}$ (Figure 1B) and immunolabelling of frozen sections with a pan laminin antibody showed that the disorganisation of the pial basement membrane apparent in $FKRP^{KD}$ mice (Figure 1E) had been restored to that of WT in the $FKRP_{MD}$ (Figure 1D and F). In order to further confirm that this strategy was successful we undertook an analysis of muscle and brain tissue from the $FKRP_{MD}$ mice using quantitative RT PCR. This showed that whilst a marked reduction in *Fkrp* transcript levels was still apparent in the muscle of $FKRP_{MD}$ mice, levels had been restored to that of wild type in the brain (Figure 1G). We previously showed that the percentage knock-down of *Fkrp* in the $FKRP^{KD}$ mouse was similar in all tissues. Here we show that the percentage knock-down of *Fkrp* in the muscle of the $FKRP_{MD}$ was similar to that seen in the brain of the $FKRP^{KD}$ at E15.5 (Figure 1H).

Reduced *Fkrp* levels in skeletal muscle are associated with a progressive muscular dystrophy

$FKRP_{MD}$ male mice were shown to have a 12 and 20 week body weight not significantly different from control mice although female body weight was reduced at 20 but not 12 weeks relative to controls (Figure 2A). The lifespan and general behaviour of $FKRP_{MD}$ mice was indistinguishable from their wild type littermates.

Haematoxylin and eosin stained sections of newborn $FKRP_{MD}$ muscle showed no evidence of muscle fibre necrosis either in the fore or hindlimb muscles (data not shown). However, by 6 weeks of age occasional areas of small basophilic regenerating fibres and inflammatory infiltrates could be seen in the $FKRP_{MD}$ gastrocnemius (Figure 2C). This feature was quite variable between individuals with some mice showing only minimal evidence of any pathology at this age. By 12 weeks of age both the gastrocnemius (Figure 2E) and the diaphragm (data not shown) of all $FKRP_{MD}$ mice exhibited fibre degeneration characterised by sarcoplasmic hyalinisation, loss of cross striations, and sarcoplasmic fragmentation and frequent groups of small, regenerative myofibres, with large, centralised nuclei and a granular pale basophilic cytoplasm (Figure 2 E). Small infiltrates of macrophages, lymphocytes and rare plasma cells, were observed to invade the interstitium and infiltrate necrotic myofibres. At 30 weeks there was evidence of an attenuation of muscle fibre degeneration and regeneration with clusters of basophilic regenerative fibres being only occasionally evident together with rare, interstitial lymphoplasmacytic foci. Representative images of the diaphragm, gastrocnemius and quadriceps at 30 weeks are shown in Figure 2 G - K.

Interestingly, the soleus of the $FKRP_{MD}$ showed evidence of only minimal damage even at 30 weeks of age, reflected by the low percentage of central nucleation which is a marker of previous rounds of degeneration and regeneration (Figure 2 L-M). This parameter nonetheless increased between 12 and 30 weeks of age in all three muscles (gastrocnemius (48.9% to 57.3%), soleus (5.6% to 20.9%) and diaphragm (32.4% to 40.7%), with a Generalised Estimating Equations model showing that age, muscle and genotype were significant interacting factors affecting the percentage of centrally nucleated muscle fibres (Figure 2 L-M). In contrast to previous findings in the dystrophin deficient *mdx* mouse, the diaphragm did not seem to be more severely affected than the limb muscles. Muscle sampled

from wild type littermates at either 12 or 30 week time points was histologically unremarkable, exhibiting normal histopathological changes for mice of this genetic background i.e. the presence of minimal, rare, interstitial, lymphoplasmacytic infiltrates.

A reduction in α-dystroglycan glycosylation is associated with an alteration in laminin α2 and α4 expression

The skeletal muscle of the $FKRP_{MD}$ mice displayed a near absence of immunolabelling with the IIH6 antibody relative to wild type littermates at 30 weeks of age (Figure 6B), with Western blotting further confirming the absence of functional glycosylation as judged by the absence of the IIH6 epitope and also showed that β-dystroglycan was unchanged (Figure 3G). Immunolabelling for laminin α2 which has previously been shown to be variably reduced in cases of LGMD2I (48), was shown to be increased on some fibres but decreased on others relative to WT controls in the $FKRP_{MD}$ at 12 weeks. Those fibres with a higher level tended to be associated with areas of increased cellular activity, whilst larger fibres showed either a slight decrease or similar levels to that of WT controls (Figure 3A-F). The application of a look up table to these images shows this variation more clearly (Figure 3H,I).

Laminin α4 has previously been shown to be up-regulated in the basement membranes of blood vessels, the perineurium of intramuscular nerves, and isolated regenerating muscle fibres of laminin α2 deficient mice (*dy/dy*) (49). In wild type controls laminin α4 localised to the capillaries, nerves and neuromuscular junctions (Figure 4A,C,D), however in the $FKRP_{MD}$ at 12 weeks of age laminin α4 was additionally increased at the sarcolemma of small groups of fibres. By 30 weeks of age a higher proportion of fibres showed laminin α4 at the sarcolemma than at earlier ages (Figure 4D,F). This was the case for each of the muscles examined (diaphragm, quadriceps and triceps). This up-regulation was not specifically associated with regenerating fibres as determined by immunolabelling with developmental myosin which only labelled very few fibres at either 12 or 30 weeks.

The overexpression of LARGE leads to a shortened lifespan and worsening of the $FKRP_{MD}$ phenotype

Previous work indicated that the upregulation of LARGE could be beneficial in the dystroglycanopathies (44,50,51). Contrary to expectation $FKRP_{MD}$ overexpressing LARGE ($FKRP_{MD}$LARGE) had a reduced lifespan in contrast to $FKRP_{MD}$ mice - a subsequent deterioration in the overall condition of $FKRP_{MD}$LARGE mice led to some mice being culled at a humane end point which was often around 27 weeks of age. $FKRP_{MD}$LARGE displayed normal behaviour, aside from an abnormal stance and a partial collapse of the leg extensor reflex, a feature not observed in the $FKRP_{MD}$ mice.

In keeping with the more severe phenotype, $FKRP_{MD}$LARGE mice displayed a more severe pathology than age-matched $FKRP_{MD}$ controls at 12 weeks as indicated by a marked variation in fibre size, centrally nucleated muscle fibres (Supplementary Figure 1) and significant increases in the number of split fibres (Figure 7D). A Generalised Estimating Equations statistical model showed that age, genotype and muscle were significant factors affecting the percentage of centrally nucleated fibres suggesting that LARGE upregulation

significantly increased the percentage of centrally nucleated fibres at both 12 and 30 weeks of age, relative to the $FKRP_{MD}$ (Figure 7). There was in addition a more pronounced expansion of the interstitium with small to moderate amounts of variably-mature fibroadipose tissue and a substantial inflammatory component, which infiltrated both the interstitium and necrotic muscle fibres and was comprised of moderate numbers of neutrophils, macrophages and lesser numbers of lymphocytes and plasma cells (Supplementary Figure 1). This was seen in all muscles examined at 12 weeks of age, including the diaphragm, gastrocnemius, tibialis anterior (TA) and soleus (Supplementary Figure 1).

In those mice that survived to 30 weeks there was a noticeable hypertrophy of many fibres, (relative to the $FKRP_{MD}$). Individual (predominantly centrally nucleated) muscle fibres were occasionally surrounded by moderate to large amounts of compact, fibrous connective tissue and infiltrates of fat (Figure 5B, D, F, H), with some muscle fibres mineralised. At this later time point as in the $FKRP_{MD}$, there was minimal degeneration and necrosis although the inflammatory infiltration was more marked with infiltration by both neutrophils and macrophages in the diaphragm and gastrocnemius. Alizarin red staining showed a marked increase in the presence of large calcium deposits in the $FKRP_{MD}$LARGE relative to the $FKRP_{MD}$ mice (Figure 5 I-K). This was the case for all the muscles examined including the soleus. Alizarin red staining was also markedly worse in the diaphragm of the $FKRP_{MD}$LARGE mice, relative to the gastrocnemius at 12 weeks of age, a difference between these muscles that was not evident in the $FKRP_{MD}$ mice at this age.

$FKRP_{MD}$LARGE mice display an increase in IIH6 labelling and laminin deposition

The glycosylation of α-DG as assessed by IIH6 immunolabelling was increased in all $FKRP_{MD}$LARGE muscles examined (diaphragm, gastrocnemius and soleus) relative to wild type mice (Figure 6 shows the gastrocnemius), and levels were comparable to that of the original LARGE transgenic line (data not shown). Laminin α2 deposition at the basement membrane was increased in $FKRP_{MD}$LARGE mice relative to $FKRP_{MD}$ mice or wild type. Whilst regenerating fibres are known to express higher levels of basement membrane proteins, this increase extended beyond the clusters of small regenerating fibres. The number of fibres with sarcolemmal labelling for laminin α4 was also increased in the $FKRP_{MD}$LARGE mice relative to $FKRP_{MD}$ mice (Figure 6). Western blot analysis of muscle at 15-20 weeks showed that transgene expression in either the wild type or $FKRP_{MD}$ gives rise to an increase in laminin binding relative to wild type confirming that expression of the transgene led to the hyperglycosylation of α-DG. (Figure 7).

$FKRP_{MD}$LARGE mice show a physiological deficit relative to the $FKRP_{MD}$

To compare the functional properties associated with a knock-down of Fkrp and how this was altered by the transgenic expression of LARGE we subjected the TA muscles of anaesthetized mice to a protocol of 10 eccentric (lengthening) contractions *in situ*. The protocol induced a 15% stretch during each of 10 maximal isometric contractions stimulated 2 minutes apart. Isometric tetanic force was measured prior to each stretch and expressed as a percentage of baseline isometric force. $FKRP_{MD}$ mice showed a similar resistance to eccentric contraction-induced injury to non-transgenic age-matched wild type controls

(101.1% and 118.5% of baseline isometric force generated in the last contraction respectively) with only a small significant drop in force after contraction 10. However, $FKRP_{MD}$LARGE showed a significant reduction in their resistance (72.5% of baseline isometric force in the last contraction) relative to controls (118.1% of baseline isometric force in the last contraction) confirming that the worsened phenotype evident on histological analysis had translated into a measurable physiological deficit (Figure 8). No significant differences were observed for the force-frequency relationship between any of the genotypes (data not shown).

Discussion

LGMD2I is one of the most frequent autosomal recessive forms of LGMD and in the UK has been reported to make up 19.1% of the total LGMD group with a prevalence of 0.43/100 000 (52,53). Whilst the spectrum of disease in the dystroglycanopathies is wide, a significant proportion of patients are affected by relatively mild limb girdle muscular dystrophies without any central nervous system involvement, making it a good target for developing therapies. In order to gain insight into the disease pathogenesis of FKRP associated muscular dystrophy we previously generated a mouse model with a knock-down in Fkrp ($FKRP^{KD}$) that displayed a muscle eye brain phenotype. Whilst this model provided insight into the eye and brain phenotype (46), it died around the time of birth due to the severity of central nervous system involvement (47) and so was less useful for investigating the consequences of a reduction in *Fkrp* on postnatal muscle growth and function and for evaluating therapeutic strategies aimed at ameliorating the skeletal muscle phenotype.

In mammals, the cortex develops in an “inside out” manner, with migration of post mitotic neurons from the proliferative neuroepithelium (ventricular zone) to the cortical plate with each layer of post-mitotic neurons forming a more superficial layer than the last (54). The majority of neuronal migration is radial and is mediated by a scaffold of radial glial cells which extend from the ventricular zone (where their cell bodies are located) to the pial basement membrane. In the present report we addressed the perinatal lethality of the $FKRP^{KD}$ mouse by crossing it with a transgenic line in which Cre recombinase is expressed under control of the Sox-1 promoter to generate $FKRP^{KD}$/Sox1Cre mice which we refer to as $FKRP_{MD}$. The Sox1 promoter is known to drive expression in the neuroectoderm early during development (55) and this cross resulted in mice with wild type *Fkrp* transcript levels in the brain, a restoration of IIH6 immunolabelling at the pial basement membrane and normal cortical architecture. Previous work has indicated that the restoration of glial rather than neuronal dystroglycan that plays a crucial role in forebrain development (56) and the restoration of the pial basement membrane and cortical organisation we observed was therefore consistent with these observations. As expected there remained an approximate 80% reduction of *Fkrp* transcript levels in the skeletal muscle which was associated with the loss of the laminin binding epitope IIH6 as previously reported for the $FKRP^{KD}$ line (21).

Despite the absence of the laminin binding IIH6 epitope from birth, the onset of muscle degeneration first occurred around 6 weeks of age in the majority of animals and by 12 weeks of age a marked pathology was evident in all $FKRP_{MD}$ mice. Western blot analysis confirmed that the IIH6 epitope was completely absent. This also resulted in the loss of

laminin binding which is consistent with previous studies in the $LARGE_{myd}$, $POMGnT_{null}$ and POMT1 mice that also report a reduction in the ability to bind laminin and develop a severe muscular dystrophy (57). In contrast, the muscle of a mouse model of FCMD (FCMD Hp^{-}) which contains a retrotransposal insertion in the mouse fukutin ortholog also failed to label with IIH6 but retained the ability to bind laminin albeit at 50% of the levels of controls. This mouse did not display any signs of a muscular dystrophy suggesting the existence of a threshold of glycosylation/laminin binding activity which was met in the FCMD mice (58) but not in the $LARGE_{myd}$ and $POMGnT_{null}$ or our $FKRP_{MD}$ mice.

All laminin isoforms with LN (Laminin N-terminal) domains play an integral role in basement membrane assembly by anchoring to cell surfaces, self polymerizing, and binding to nidogen and collagen IV (1). Laminin 211 is the major laminin isoform present in skeletal muscle and is reduced albeit not invariably in the skeletal muscle of dystroglycanopathy patients. A variation in laminin α2 immunolabelling was also observed in $FKRP_{MD}$ mice at 12 weeks with higher levels of labelling apparent on small regenerating fibres whilst the majority of larger fibres either showed similar levels to that of controls or a reduction implying that a reduction in glycosylation may influence the turnover and/or stability of laminin 211 in the basement membrane of mature muscle fibres. Interestingly, there was no obvious reduction in perlecan in the $FKRP_{MD}$ mice when compared to wildtype mice (data not shown) despite previous reports of a reduction in the perlecan-binding activity and its mis-localisation in the brains of $Large_{myd}$ and dystroglycan null mice (59). However, it may be that laminin α2 rather than perlecan is the main binding partner for α-dystroglycan in muscle, indeed the binding properties of α-dystroglycan are known to be different in brain and muscle (60).

We observed a redistribution of laminin α4 in the $FKRP_{MD}$ muscle which has also been reported in laminin α2 deficient mice (49). Laminin α4 normally locates to the basement membranes of blood vessels, the endoneurium of the intramuscular nerves, and the neuromuscular junction in neonatal skeletal muscle (49). In adult muscle it locates to the perineurium of adult peripheral nerve. Laminin α4 lacks the ability to self-polymerise (61) due to the absence of the N-terminal domain, and consequently has the potential to interfere with basal lamina formation where laminin α2 is a major component. It also displays a low affinity binding for α-dystroglycan, sulfatides, and integrins α6β1 and α7β1 (62), properties that suggest it may be an ineffective substitute for laminin α2. However, the up-regulation of laminin α4, which is also a feature of laminin α2 deficiency may nonetheless be of functional significance since recent work in the zebra fish suggests that its up-regulation in damaged fibres contributes to fibre survival (63). Interestingly, an increase in the number of fibres with laminin α4 at the sarcolemma was observed to increase with age in the $FKRP_{MD}$, implying that a similar scenario may apply to our mice.

LARGE is a bifunctional glycosyltransferase thought to be essential for conferring α-dystroglycan with the ability to bind laminin. The over-expression of LARGE has been shown to increase-DG glycosylation in both wild type and cells from dystroglycanopathy patients, irrespective of their primary gene defect (44). Whilst more recent work now demonstrates that the ability of LARGE to hyperglycosylate α-dystroglycan is dependent on the availability of O-mannosyl phosphate acceptor sites and correlates with the severity of

the clinical phenotype (32); this strategy is still considered as being potentially useful for a wide range of patients. Furthermore, the viral delivery of LARGE to skeletal muscle in animal models of dystroglycanopathy has been reported to have identical effects *in vivo*, suggesting that the restoration of functional glycosylation may be a valuable therapeutic approach in this group of disorders (44,58). We previously generated a number of transgenic lines overexpressing LARGE (45) and have now crossed one of these lines with our $FKRP_{MD}$ mice. On a wild type background the up-regulation of LARGE is not associated with any muscle fibre degeneration but there is a mild loss of force upon eccentric exercise in the TA of older animals (45), suggesting some form of subtle abnormality in basement membrane turnover occurs over an extended time period (64). However, when we crossed the $FKRP_{MD}$ line with the LARGE transgenic the pathology of the $FKRP_{MD}$ phenotype worsened with an increased percentage of centrally nucleated fibres in all the muscles examined relative to the $FKRP_{MD}$. Additional features such as calcium deposits, evidence of fibrosis and replacement of muscle fibres by adipocytes were also more evident in the presence of the LARGE transgene and the soleus muscle which was largely spared in the $FKRP_{MD}$ showed clear evidence of pathology in the presence of the LARGE transgene. The promoter driving the LARGE transgene expresses at equivalent levels in both slow and fast fibres therefore these observations reflect a differential pattern of muscle involvement in the $FKRP_{MD}$.

Whilst there are several differences between our study and those which previously indicated that the up-regulation of LARGE would be beneficial such as the method of gene delivery, promoter used to drive expression, and animal model, the most significant difference relates to the timing over which LARGE was overexpressed, and the duration of the period of observation. For example, LARGE was introduced into the $Large^{myd}$, $POMGnT1^{-/-}$ and FCMD Hp^{-} mice via AAV vectors at postnatal data 2-4 and then evaluated 4 weeks later (44,58). More recently Yu et al (50) injected AAV9-LARGE (expression driven by the β-actin promoter) via into the newborn heart and adult tail vein of POMGnT1null and $LARGE_{myd}$ mice and looked at expression at 2 months (newborn injections) and 1 month (adult tail vein injections) later. These authors noted significant improvement of the histological appearance of the muscle and amelioration of the phenotype. Barresi et al (44) also administered *LARGE* to older $Large^{myd}$ mice, aged between 12 days and 5 weeks but reported that this was associated with muscle inflammation and a loss of IIH6 immunolabelling (*LARGE* up-regulation) as the mice aged.

These findings are in marked contrast to those of our own using transgenesis and would seem to imply that the time period over which LARGE is up-regulated and/or the stage of development that it is initiated determine the outcome. Here we have shown that despite the restoration of laminin binding in the $FKRP_{MD}$LARGE there was a significant loss of force in response to eccentric exercise which was not seen in the $FKRP_{MD}$ confirming that the overexpression of LARGE had worsened the phenotype as indicated by the histological analyses. The reasons for this remain unclear however, it is possible that on a disease background, specifically one in which the glycosylation of α-dystroglycan is reduced or absent, LARGE not only targets additional proteins, the hyperglycosylation of which is detrimental to muscle, but may also lead to a functionally relevant alteration in the glycosylation pattern of α-DG itself. In support of these two concepts it has previously been

shown that LARGE over-expression in α-DG-deficient cells leads to the expression of the IIH6 epitope (65) and that LARGE acts not only on the *O*-mannose glycans but also complex *N*-glycans and mucin *O*-GalNAc (N-Acetylgalactosamine) glycans of α-DG (66). Previous work in ES (Embryonic Stem) cells indicates that neither integrin nor dystroglycan are individually required for assembly of the basement membrane but they do regulate both their own expression and that of other basement membrane components (67). It is therefore possible that this system of regulation is perturbed by an altered pattern of α-dystroglycan glycosylation, perhaps by compromising the turnover process of the basement membrane. Finally it should also be noted that as a consequence of the transgenic approach adopted here, the $FKRP_{MD}$LARGE mice are on a different background to the $FKRP_{MD}$ mouse. However, we consider this an unlikely cause of the worsened phenotype since histological evaluation of wildtype *LARGE* overexpressing mice on this new genetic background failed to identify any evidence of a dystrophic pathology.

Our work reports the first transgenic up-regulation of LARGE on a disease background. Whilst the onset of disease in the $FKRP_{MD}$LARGE mice was not markedly different to the $FKRP_{MD}$, suggesting that the over-expression of LARGE did not adversely affect the early stages of muscle development, several aspects of the disease process were significantly worse. The reasons for this are unclear at the present time, but emphasise the value of determining the effect of overexpression on a disease background over an extended period and suggest that any therapeutic approach involving LARGE up-regulation requires careful management.

Materials and Methods

Generation of FKRP-Neo$^{Tyr307Asn+/+Sox1Cre}$ mice ($FKRP_{MD}$)

All animal experiments were carried out under license from the Home Office (UK) in accordance with The Animals (Scientific Procedures) Act 1986 and were approved by Royal Veterinary College ethical committee. The FKRP-Neo$^{Tyr307Asn+/+}$ ($FKRP^{KD}$) mouse colony (47) was crossed with a second transgenic line expressing *Cre recombinase* throughout the developing neural tube under the Sox1 promoter (a kind gift from Professor Liz Robertson, Sir William Dunn School of Pathology, Oxford U.K.) (68). Briefly FKRP-Neo$^{Tyr307Asn+/-}$ were crossed with Sox1Cre mice and the resulting FKRP-NeoTyr$^{307Asn+/-Sox1Cre}$ mice were bred with FKRP-Neo$^{Tyr307Asn+/-}$ mice which generated FKRP-Neo$^{Tyr307Asn+/+Sox1Cre}$ mice, referred to as $FKRP_{MD}$. Thus, the first cross introduced the Sox1Cre transgene into the background of the $FKRP^{KD}$ colony, while the second first generation cross generated the $FKRP_{MD}$ offspring at a frequency of approximately 7%. $FKRP_{MD}$ mice are fertile and breeding them with FKRP-Neo$^{Tyr307Asn+/-}$ mice increased the incidence of mice to approximately 14%. However, pairing two FKRP-Neo$^{Tyr307Asn+/-Sox1Cre}$ heterozygote mice resulted in high pre-weaning losses, with a number of offspring suffering from hydrocephalus.

Generation of FKRP-Neo$^{Tyr307Asn+/+Sox1CreLARGE}$ ($FKRP_{MD}$LARGE)

The following strategy was used to generate $FKRP_{MD}$, $FKRP^{KD}$ and $FKRP_{MD}$ LARGE mice. FKRP-Neo$^{Tyr307Asn+/-Sox1Cre}$ mice were crossed with a transgenic mouse line (LV5)

overexpressing human LARGE (45) to introduce the LARGE transgene into the background of the $FKRP_{MD}$ mice. FKRP-$Neo^{Tyr307Asn+/-Sox1CreLARGE}$ mice were then crossed with FKRP-$Neo^{Tyr307Asn+/-}$ to generate FKRP-$Neo^{Tyr307Asn+/+Sox1CreLARGE}$ mice, henceforth referred to as $FKRP_{MD}$LARGE mice.

Genotyping $FKRP_{MD}$ offspring

Offspring were genotyped by PCR analysis using either ear or tail biopsies. Genomic DNA from the mouse tissue was prepared by digestion in Direct PCR Lysis Ear or Tail buffer (Eurogentec) respectively containing 0.2mg/mL Proteinase K (Roche Diagnostics) at 55°C overnight. The Proteinase K was heat inactivated at 85°C for 30 minutes and PCR was performed with the crude DNA lysate using Biomix Red PCR Kit (Bioline) with the following multiplex primers for Fkrp (FKRP-F: CTAGGAGGTTGAGGATGATGG, FKRP-R: GTTGTGCTTAAACCACCTTC, and FKRP-NeoF:GGTGGATTAGATAAATGC), Cre recombinase (Cre-F: CCCAGGCTAAGTGCCTTCTC and Cre-R: CCAGGTTCGTTCACTCATGG) and *LARGE* (Large-F:TAATACGACTCACTATAGGG Large-R: AAGGTTCTCGCTGTCTCC).

Histology and Immunocytochemistry

For standard histochemistry, newborn mice were collected and fixed in Bouins (Sigma) and transferred to 70% ethanol prior to processing and embedding in paraffin wax. Samples were serially sectioned at 5μm, with sections collected onto charged slides (Superfrost Plus, VWR), rehydrated and stained with haematoxylin and eosin, using standard methods. For immunohistochemistry sections were deparaffinised and rehydrated prior to incubation with anti α-dystroglycan (IIH6, Millipore) diluted in phosphate buffered saline containing 0.05% tween 20 (Sigma) for 1 hour at room temperature. Visualisation of the IIH6 was performed using the Envision system (DAKO).

Alternatively, muscle and brain samples were frozen in isopentane cooled in liquid nitrogen and 10μm sections were cut using a Bright Cryostat. These were then stained with haematoxylin and eosin using standard methods to evaluate general tissue pathology and calculate the percentage of centrally located nuclei. Additionally, Alizarin Red staining was performed to identify calcium deposits. Images of newborn mouse heads and muscles stained with these histochemical methods were digitally captured using a DM4000B upright microscope (Leica, Germany) interfaced with a DC500 colour camera (Leica) using the Leica Application Suite (Leica Microsystems) software provided and compiled into figures using Photoshop CS4 or CS5 (Adobe, U.S.A.). Figures were compiled using Photoshop CS (Adobe, U.S.A.). All observations are based on a minimum of n=3 (of either sex), and representative images are shown. Counts of centrally nucleated muscle fibres were made across an entire section from each individual mouse muscle (n=3 for wildtype, $FKRP_{MD}$ and $FKRP_{MD}$LARGE mice at 12 and 30 weeks of age) randomly chosen from the mid-region of each muscle, with the total number of fibres counted numbering approximately 500, 1500 and 2000 muscle fibres in the soleus, diaphragm and gastrocnemius respectively. The incidence of split muscle fibres was based on counts of approximately 2000 muscle fibres across an entire section from the mid-belly region of 12 week old wildtype, $FKRP_{MD}$ and $FKRP_{MD}$LARGE gastrocnemius (n=3 for all genotypes).

For immunohistochemical analysis of muscle and brain, cryosections were immunolabelled with rabbit anti pan-laminin (Sigma-Aldrich), rat anti laminin α2 (4H8, Abcam), goat anti-laminin α4 (R&D Systems) and the IIH6 antibody against a glycosylated epitope of α-DG (Millipore). This was followed by anti-rat/rabbit/goat tagged with Alexa 488 or 594 (Molecular Probes) for 30 minutes, with the exception of IIH6 which was labelled with anti-IgM biotinylated antibody (30 minutes) followed by streptavidin conjugated with Alexa 488/594 (30 minutes). Nuclei were stained with Hoechst 33342 (Sigma-Aldrich). All dilutions and washes were made in phosphate buffered saline. Sections were mounted in aqueous mountant and viewed with epifluorescence using a DM4000B upright microscope (Leica, Germany). Images were digitally captured with an Axiovision mRM monochrome camera, (Zeiss, UK) and compiled using Photoshop CS (Adobe, U.S.A.). Where direct comparisons have been made, fluorescent images were captured with equal exposure and have had equal scaling applied. All observations are based on a minimum of n=3 (of either sex), representative images are shown.

qRTPCR analysis

Brain and muscle were dissected out and homogenised with liquid nitrogen using a mortar and pestle and the lysate passed through a QiaShredder®(Qiagen). RNA was isolated from the homogenised tissue using an RNeasy®kit (Qiagen) and for muscle RNeasy® Fibrous Tissue Kit (Qiagen) eluted with 30μl RNase free H_2O. 1μg of RNA was reverse transcribed with Superscript®III Platinum for qRT-PCR kit (Invitrogen). qRT-PCR was performed on a 7500 FAST Real-Time PCR system (Applied Biosystems) using aFAM$^{(tm)}$ reporter dye system. For each reaction 0.8μl of cDNA was used as template in a PCR mix consisting of 1μl of primer mix, 10 ul TaqMan Universal PCR Mastermix (Applied Biosystems) and 8.2μl H_2O. The primers for the gene expression assays were sourced commercially from Applied Biosystems (*FKRP* Mm00557870_mL, *GAPDH* Mm99999915_gL). Each experiment represents a minimum of n=4 (of either sex) and all reactions were performed in triplicate.

Western blotting and laminin overlay assay

Cell proteins were extracted in sample buffer consisting of 75 mM Tris–HCl, 1% SDS, 2-mercaptoethanol, plus a cocktail of protease inhibitors (Roche). 30μg of soluble proteins were resolved using a NuPage Pre-cast gel (3–8% Tris-acetate; Invitrogen, USA) and then transferred electrophoretically to nitrocellulose membrane (Hybond-PVDF, GE Healthcare, UK. Nitrocellulose strips were blocked in 5% dried non fat milk in phosphate-buffered saline buffer, and then probed with the primary antibodies: anti mouse α-DG IIH6 (Millipore UK,cat,05-593) anti-mouse β-DG (Vector Labs, UK), at room temperature for 1 hour. After washing they were incubated with the appropriate HRP conjugated secondary antibody for one hour: anti-mouse-IgM or anti-mouse-IgG (both from Jackson ImmunoResearch). After washing, membranes were visualized using chemiluminescence (ECL+Plus, GE Healthcare, UK). For the laminin overlay assay, nitrocellulose membranes were blocked for 1 hour in laminin binding buffer (LBB: 10 mM triethanolamine, 140 mM NaCl, 1 mM $MgCl_2$, 1 mM $CaCl_2$, pH 7.6) containing 5% non-fat dry milk followed by incubation of mouse Engelbreth-Holm-Swarm laminin (Invitrogen,USA) overnight at 4°C in LBB. Membranes were washed and incubated with anti rabbit laminin (Sigma, USA)

followed by HRP-anti rabbit IgG (Jackson ImmunoResearch, USA). Blots were visualized using chemiluminescence (ECL+Plus, GE Healthcare,UK).

In situ/vivo muscle electrophysiology

Mice were surgically prepared as described previously (69,70). Contractions were stimulated in the TA muscle *in situ* via the surgically isolated common peroneal nerve. The TA muscle underwent a series of 5 submaximal isometric contractions as a warm up. Isometric force measurements were made over a range of stimulating frequencies and maximum isometric tetanic force (P_0) was determined from the plateau of the force–frequency curve (20). After completing the final isometric contraction the optimum length (Lo) was measured with digital callipers and the muscle was allowed to rest for 5 min before the eccentric contraction protocol was initiated. A tetanic contraction was induced using a stimulus of 120 Hz (the frequency that resulted in P_0 without causing fatigue during the contraction) for 700 ms. During the last 200 ms of this contraction, the muscle was stretched by 15% of L_o at a velocity of 0.75 $L_o s^{-1}$ and relaxed at -0.75$L_o s^{-1}$. The isometric tension recorded prior to the first stretch was used as a baseline. The muscle was then subjected to 10 eccentric contractions each separated by a 2 min rest period to avoid the confounding effect of muscle fatigue. The isometric tension prior to each stretch was recorded and expressed as a percentage of the baseline tension (69). The mouse was then euthanized and the muscle was carefully removed and weighed.

Statistical analyses

Body weights were analysed with a Linear Mixed Effects Model and central nucleation counts were analysed with a General Estimating Equations model, both performed using SPSS Statistics (IBM, U.S.A). The incidence of split fibres was analysed with a one-tailed Mann-Whitney test, Muscle physiology data were analysed using a Repeated Measures One-way ANOVA with Tukey's *post-hoc* comparison.

Supplementary Material

Refer to Web version on PubMed Central for supplementary material.

Acknowledgements

We would like to acknowledge the kind gift of the Sox1Cre recombinase expressing mice from Professor Liz Robertson, Sir William Dunn School of Pathology, Oxford U.K and the excellent technical assistance of Alice Nettleton. We also thank Drs. Anne Rutkowski and Claudia Mitchell for their helpful discussions during the course of this work. We gratefully acknowledge the support of Cure CMD (Congenital Muscular Dystrophy), the Muscular Dystrophy Association of America (MDA) and Association Francaise contres les Myopathies (AFM). FM is supported by the Great Ormond Street Children's Charity and the Biomedical Research Centre and CW is supported by a Medical Research Council studentship.

Abbreviations

α-DG	α-dystroglycan
AAV	Adeno-Associated Virus
B3GNT1	Beta-1,3-N-Acetylglucosaminyltransferase 1

Europe PMC Funders Author Manuscripts

Europe PMC Funders Author Manuscripts

CMD	Congenital Muscular Dystrophy
DG	Dystroglycan
DOLK	Dolichol Kinase
DPM2	Dolichyl-Phosphate Mannosyltransferase Polypeptide 2
DPM3	Dolichyl-Phosphate Mannosyltransferase Polypeptide 3
ES	Embryonic Stem
FCMD	Fukuyama Congenital Muscular Dystrophy
FKT	Fukutin
FKRP	Fukutin Related Protein
$FKRP^{KD}$	FKRP knock down
$FKRP_{MD}$	FKRP muscular dystrophy
GalNAc	N-Acetylgalactosamine
GMPPB	GDP-mannose pyrophosphorylase B
GTDC2	Glycosyltransferase-Like Domain Containing 2
ISPD	Isoprenoid Synthase Domain Containing
LARGE	Like-acetylglucosaminyltransferase
LG	Laminin globular
LN	Laminin N-terminal
LGMD	Limb girdle muscular dystrophy
MDC1D	Congenital Muscular Dystrophy Type 1D
MEB	Muscle Eye Brain Disease
POMT1	Protein O-mannosyl-transferase 1
POMT2	Protein O-mannosyl-transferase 2
POMGnT1	Protein O-mannose beta-1,2-N-acetylglucosaminyltransferase
RT PCR	Reverse Transcriptase Polymerase Chain Reaction
Sox1	Sex determining region Y-box 1
SGK196	Sugen Kinase 196
TA	Tibialis Anterior
TMEM5	Transmembrane Protein 5

WWS Walker-Warburg Syndrome

Reference List

1. Yurchenco PD, Patton BL. Developmental and pathogenic mechanisms of basement membrane assembly. Curr Pharm Des. 2009; 15:1277–1294. [PubMed: 19355968]
2. Henry MD, Williamson RA, Campbell KP. Analysis of the role of dystroglycan in early postimplantation mouse development. Ann N Y Acad Sci. 1998; 857:256–259. [PubMed: 9917851]
3. Henry MD, Campbell KP. A role for dystroglycan in basement membrane assembly. Cell. 1998; 95:859–870. [PubMed: 9865703]
4. Yurchenco PD, Amenta PS, Patton BL. Basement membrane assembly, stability and activities observed through a developmental lens. Matrix Biol. 2004; 22:521–538. [PubMed: 14996432]
5. Yurchenco PD, Cheng YS, Campbell K, Li S. Loss of basement membrane, receptor and cytoskeletal lattices in a laminin-deficient muscular dystrophy. J Cell Sci. 2004; 117:735–742. [PubMed: 14734655]
6. Durbeej M, Larsson E, Ibraghimov-Beskrovnaya O, Roberds SL, Campbell KP, Ekblom P. Non-muscle alpha-dystroglycan is involved in epithelial development. J Cell Biol. 1995; 130:79–91. [PubMed: 7790379]
7. Michele DE, Barresi R, Kanagawa M, Saito F, Cohn RD, Satz JS, Dollar J, Nishino I, Kelley RI, Somer H, et al. Post-translational disruption of dystroglycan-ligand interactions in congenital muscular dystrophies. Nature. 2002; 418:417–422. [PubMed: 12140558]
8. Ervasti JM, Burwell AL, Geissler AL. Tissue-specific heterogeneity in alpha-dystroglycan sialoglycosylation. Skeletal muscle alpha-dystroglycan is a latent receptor for Vicia villosa agglutinin b4 masked by sialic acid modification. J Biol Chem. 1997; 272:22315–22321. [PubMed: 9268382]
9. Ervasti JM, Campbell KP. A role for the dystrophin-glycoprotein complex as a transmembrane linker between laminin and actin. J Cell Biol. 1993; 122:809–823. [PubMed: 8349731]
10. Peng HB, Ali AA, Daggett DF, Rauvala H, Hassell JR, Smalheiser NR. The relationship between perlecan and dystroglycan and its implication in the formation of the neuromuscular junction. Cell Adhes Commun. 1998; 5:475–489. [PubMed: 9791728]
11. Bowe MA, Deyst KA, Leszyk JD, Fallon JR. Identification and purification of an agrin receptor from Torpedo postsynaptic membranes: a heteromeric complex related to the dystroglycans. Neuron. 1994; 12:1173–1180. [PubMed: 8185951]
12. Campanelli JT, Roberds SL, Campbell KP, Scheller RH. A role for dystrophin-associated glycoproteins and utrophin in agrin-induced AChR clustering. Cell. 1994; 77:663–674. [PubMed: 8205616]
13. Gee SH, Montanaro F, Lindenbaum MH, Carbonetto S. Dystroglycan-alpha, a dystrophin-associated glycoprotein, is a functional agrin receptor. Cell. 1994; 77:675–686. [PubMed: 8205617]
14. Sugita S, Saito F, Tang J, Satz J, Campbell K, Sudhof TC. A stoichiometric complex of neurexins and dystroglycan in brain. J Cell Biol. 2001; 154:435–445. [PubMed: 11470830]
15. Sato S, Omori Y, Katoh K, Kondo M, Kanagawa M, Miyata K, Funabiki K, Koyasu T, Kajimura N, Miyoshi T, et al. Pikachurin, a dystroglycan ligand, is essential for photoreceptor ribbon synapse formation. Nat Neurosci. 2008; 11:923–931. [PubMed: 18641643]
16. Wright KM, Lyon KA, Leung H, Leahy DJ, Ma L, Ginty DD. Dystroglycan organizes axon guidance cue localization and axonal pathfinding. Neuron. 2012; 76:931–944. [PubMed: 23217742]
17. Hohenester E, Tisi D, Talts JF, Timpl R. The crystal structure of a laminin G-like module reveals the molecular basis of alpha-dystroglycan binding to laminins, perlecan, and agrin. Mol Cell. 1999; 4:783–792. [PubMed: 10619025]
18. Tisi D, Talts JF, Timpl R, Hohenester E. Structure of the C-terminal laminin G-like domain pair of the laminin alpha2 chain harbouring binding sites for alpha-dystroglycan and heparin. EMBO J. 2000; 19:1432–1440. [PubMed: 10747011]

19. Michele DE, Campbell KP. Dystrophin-glycoprotein complex: post-translational processing and dystroglycan function. J Biol Chem. 2003; 278:15457–15460. [PubMed: 12556455]
20. Yoshida-Moriguchi T, Yu L, Stalnaker SH, Davis S, Kunz S, Madson M, Oldstone MB, Schachter H, Wells L, Campbell KP. O-mannosyl phosphorylation of alpha-dystroglycan is required for laminin binding. Science. 2010; 327:88–92. [PubMed: 20044576]
21. Ackroyd MR, Skordis L, Kaluarachchi M, Godwin J, Prior S, Fidanboylu M, Piercy RJ, Muntoni F, Brown SC. Reduced expression of fukutin related protein in mice results in a model for fukutin related protein associated muscular dystrophies. Brain. 2009; 132:439–451. [PubMed: 19155270]
22. Beltran-Valero DB, Currier S, Steinbrecher A, Celli J, van Beusekom E, van der ZB, Kayserili H, Merlini L, Chitayat D, Dobyns WB, et al. Mutations in the O-mannosyltransferase gene POMT1 give rise to the severe neuronal migration disorder Walker-Warburg syndrome. Am J Hum Genet. 2002; 71:1033–1043. [PubMed: 12369018]
23. van Reeuwijk J, Janssen M, van den EC, de Beltran-Valero BD, Sabatelli P, Merlini L, Boon M, Scheffer H, Brockington M, Muntoni F, et al. POMT2 mutations cause alpha-dystroglycan hypoglycosylation and Walker-Warburg syndrome. J Med Genet. 2005; 42:907–912. [PubMed: 15894594]
24. Yoshida A, Kobayashi K, Manya H, Taniguchi K, Kano H, Mizuno M, Inazu T, Mitsuhashi H, Takahashi S, Takeuchi M, et al. Muscular dystrophy and neuronal migration disorder caused by mutations in a glycosyltransferase, POMGnT1. Dev Cell. 2001; 1:717–724. [PubMed: 11709191]
25. Longman C, Brockington M, Torelli S, Jimenez-Mallebrera C, Kennedy C, Khalil N, Feng L, Saran RK, Voit T, Merlini L, et al. Mutations in the human LARGE gene cause MDC1D, a novel form of congenital muscular dystrophy with severe mental retardation and abnormal glycosylation of alpha-dystroglycan. Hum Mol Genet. 2003; 12:2853–2861. [PubMed: 12966029]
26. van Reeuwijk J, Grewal PK, Salih MA, de Beltran-Valero BD, McLaughlan JM, Michielse CB, Herrmann R, Hewitt JE, Steinbrecher A, Seidahmed MZ, et al. Intragenic deletion in the LARGE gene causes Walker-Warburg syndrome. Hum Genet. 2007; 121:685–690. [PubMed: 17436019]
27. Grewal PK, Hewitt JE. Mutation of Large, which encodes a putative glycosyltransferase, in an animal model of muscular dystrophy. Biochim Biophys Acta. 2002; 1573:216–224. [PubMed: 12417403]
28. Toda T. [Fukutin, a novel protein product responsible for Fukuyama-type congenital muscular dystrophy]. Seikagaku. 1999; 71:55–61. [PubMed: 10067123]
29. Brockington M, Blake DJ, Prandini P, Brown SC, Torelli S, Benson MA, Ponting CP, Estournet B, Romero NB, Mercuri E, et al. Mutations in the fukutin-related protein gene (FKRP) cause a form of congenital muscular dystrophy with secondary laminin alpha2 deficiency and abnormal glycosylation of alpha-dystroglycan. Am J Hum Genet. 2001; 69:1198–1209. [PubMed: 11592034]
30. Brockington M, Yuva Y, Prandini P, Brown SC, Torelli S, Benson MA, Herrmann R, Anderson LV, Bashir R, Burgunder JM, et al. Mutations in the fukutin-related protein gene (FKRP) identify limb girdle muscular dystrophy 2I as a milder allelic variant of congenital muscular dystrophy MDC1C. Hum Mol Genet. 2001; 10:2851–2859. [PubMed: 11741828]
31. Lefeber DJ, Schonberger J, Morava E, Guillard M, Huyben KM, Verrijp K, Grafakou O, Evangeliou A, Preijers FW, Manta P, et al. Deficiency of Dol-P-Man synthase subunit DPM3 bridges the congenital disorders of glycosylationwith the dystroglycanopathies. Am J Hum Genet. 2009; 85:76–86. [PubMed: 19576565]
32. Willer T, Lee H, Lommel M, Yoshida-Moriguchi T, de Bernabe DB, Venzke D, Cirak S, Schachter H, Vajsar J, Voit T, et al. ISPD loss-of-function mutations disrupt dystroglycan O-mannosylation and cause Walker-Warburg syndrome. Nat Genet. 2012
33. Cirak S, Foley AR, Herrmann R, Willer T, Yau S, Stevens E, Torelli S, Brodd L, Kamynina A, Vondracek P, et al. ISPD gene mutations are a common cause of congenital and limb-girdle muscular dystrophies. Brain. 2013; 136:269–281. [PubMed: 23288328]
34. Manzini MC, Tambunan DE, Hill RS, Yu TW, Maynard TM, Heinzen EL, Shianna KV, Stevens CR, Partlow JN, Barry BJ, et al. Exome sequencing and functional validation in zebrafish identify GTDC2 mutations as a cause of Walker-Warburg syndrome. Am J Hum Genet. 2012; 91:541–547. [PubMed: 22958903]

35. Vuillaumier-Barrot S, Bouchet-Seraphin C, Chelbi M, Devisme L, Quentin S, Gazal S, Laquerriere A, Fallet-Bianco C, Loget P, Odent S, et al. Identification of mutations in TMEM5 and ISPD as a cause of severe cobblestone lissencephaly. Am J Hum Genet. 2012; 91:1135–1143. [PubMed: 23217329]
36. Buysse K, Riemersma M, Powell G, van RJ, Chitayat D, Roscioli T, Kamsteeg EJ, van den Elzen C, van BE, Blaser S, et al. Missense mutations in beta-1,3-N-acetylglucosaminyltransferase 1 (B3GNT1) cause Walker-Warburg syndrome. Hum Mol Genet. 2013; 22:1746–1754. [PubMed: 23359570]
37. Lefeber DJ, de Brouwer AP, Morava E, Riemersma M, Schuurs-Hoeijmakers JH, Absmanner B, Verrijp K, van den Akker WM, Huijben K, Steenbergen G, et al. Autosomal recessive dilated cardiomyopathy due to DOLK mutations results from abnormal dystroglycan O-mannosylation. PLoS Genet. 2011; 7:e1002427. [PubMed: 22242004]
38. Yoshida-Moriguchi T, Willer T, Anderson ME, Venzke D, Whyte T, Muntoni F, Lee H, Nelson SF, Yu L, Campbell KP. SGK196 Is a Glycosylation-Specific O-Mannose Kinase Required for Dystroglycan Function. Science. 2013
39. Carss KJ, Stevens E, Foley AR, Cirak S, Riemersma M, Torelli S, Hoischen A, Willer T, van SM, Moore SA, et al. Mutations in GDP-Mannose Pyrophosphorylase B Cause Congenital and Limb-Girdle Muscular Dystrophies Associated with Hypoglycosylation of alpha-Dystroglycan. Am J Hum Genet. 2013; 93:29–41. [PubMed: 23768512]
40. Brown SC, Torelli S, Brockington M, Yuva Y, Jimenez C, Feng L, Anderson L, Ugo I, Kroger S, Bushby K, et al. Abnormalities in alpha-dystroglycan expression in MDC1C and LGMD2I muscular dystrophies. Am J Pathol. 2004; 164:727–737. [PubMed: 14742276]
41. Xu L, Lu PJ, Wang CH, Keramaris E, Qiao C, Xiao B, Blake DJ, Xiao X, Lu QL. Adeno-associated virus 9 mediated FKRP gene therapy restores functional glycosylation of alpha-dystroglycan and improves muscle functions. Mol Ther. 2013 Jul 2. 2013.
42. Kanagawa M, Yu CC, Ito C, Fukada SI, Hozoji-Inada M, Chiyo T, Kuga A, Matsuo M, Sato K, Yamaguchi M, et al. Impaired viability of muscle precursor cells in muscular dystrophy with glycosylation defects and amelioration of its severe phenotype by limited gene expression. Hum Mol Genet. 2013; 22:3003–3015. [PubMed: 23562821]
43. Inamori K, Yoshida-Moriguchi T, Hara Y, Anderson ME, Yu L, Campbell KP. Dystroglycan function requires xylosyl- and glucuronyltransferase activities of LARGE. Science. 2012; 335:93–96. [PubMed: 22223806]
44. Barresi R, Michele DE, Kanagawa M, Harper HA, Dovico SA, Satz JS, Moore SA, Zhang W, Schachter H, Dumanski JP, et al. LARGE can functionally bypass alpha-dystroglycan glycosylation defects in distinct congenital muscular dystrophies. Nat Med. 2004; 10:696–703. [PubMed: 15184894]
45. Brockington M, Torelli S, Sharp PS, Liu K, Cirak S, Brown SC, Wells DJ, Muntoni F. Transgenic overexpression of LARGE induces alpha-dystroglycan hyperglycosylation in skeletal and cardiac muscle. PLoS ONE. 2010; 5:e14434. [PubMed: 21203384]
46. Ackroyd MR, Whitmore C, Prior S, Kaluarachchi M, Nikolic M, Mayer U, Muntoni F, Brown SC. Fukutin-related protein alters the deposition of laminin in the eye and brain. J Neurosci. 2011; 31:12927–12935. [PubMed: 21900571]
47. Ackroyd MR, Skordis L, Kaluarachchi M, Godwin J, Prior S, Fidanboylu M, Piercy RJ, Muntoni F, Brown SC. Reduced expression of fukutin related protein in mice results in a model for fukutin related protein associated muscular dystrophies. Brain. 2009; 132:439–451. [PubMed: 19155270]
48. Yamamoto LU, Velloso FJ, Lima BL, Fogaca LL, de P F, Vieira NM, Zatz M, Vainzof M. Muscle protein alterations in LGMD2I patients with different mutations in the Fukutin-related protein gene. J Histochem Cytochem. 2008; 56:995–1001. [PubMed: 18645206]
49. Ringelmann B, Roder C, Hallmann R, Maley M, Davies M, Grounds M, Sorokin L. Expression of laminin alpha1, alpha2, alpha4, and alpha5 chains, fibronectin, and tenascin-C in skeletal muscle of dystrophic 129ReJ dy/dy mice. Exp Cell Res. 1999; 246:165–182. [PubMed: 9882526]
50. Yu M, He Y, Wang K, Zhang P, Zhang S, Hu H. Adeno-Associated Viral-Mediated LARGE Gene Therapy Rescues the Muscular Dystrophic Phenotype in Mouse Models of Dystroglycanopathy. Hum Gene Ther. 2013; 24:317–330. [PubMed: 23379513]

51. Hewitt JE. LARGE enzyme activity deciphered: a new therapeutic target for muscular dystrophies. Genome Med. 2012; 4:23. [PubMed: 22458537]
52. Muntoni F, Torelli S, Brockington M. Muscular dystrophies due to glycosylation defects. Neurotherapeutics. 2008; 5:627–632. [PubMed: 19019316]
53. Norwood FL, Harling C, Chinnery PF, Eagle M, Bushby K, Straub V. Prevalence of genetic muscle disease in Northern England: in-depth analysis of a muscle clinic population. Brain. 2009; 132:3175–3186. [PubMed: 19767415]
54. Gupta A, Tsai LH, Wynshaw-Boris A. Life is a journey: a genetic look at neocortical development. Nat Rev Genet. 2002; 3:342–355. [PubMed: 11988760]
55. Wood HB, Episkopou V. Comparative expression of the mouse Sox1, Sox2 and Sox3 genes from pre-gastrulation to early somite stages. Mech Dev. 1999; 86:197–201. [PubMed: 10446282]
56. Satz JS, Ostendorf AP, Hou S, Turner A, Kusano H, Lee JC, Turk R, Nguyen H, Ross-Barta SE, Westra S, et al. Distinct functions of glial and neuronal dystroglycan in the developing and adult mouse brain. J Neurosci. 2010; 30:14560–14572. [PubMed: 20980614]
57. Holzfeind PJ, Grewal PK, Reitsamer HA, Kechvar J, Lassmann H, Hoeger H, Hewitt JE, Bittner RE. Skeletal, cardiac and tongue muscle pathology, defective retinal transmission, and neuronal migration defects in the Large(myd) mouse defines a natural model for glycosylation-deficient muscle - eye - brain disorders. Hum Mol Genet. 2002; 11:2673–2687. [PubMed: 12354792]
58. Kanagawa M, Nishimoto A, Chiyonobu T, Takeda S, Miyagoe-Suzuki Y, Wang F, Fujikake N, Taniguchi M, Lu Z, Tachikawa M, et al. Residual laminin-binding activity and enhanced dystroglycan glycosylation by LARGE in novel model mice to dystroglycanopathy. Hum Mol Genet. 2009; 18:621–631. [PubMed: 19017726]
59. Kanagawa M, Michele DE, Satz JS, Barresi R, Kusano H, Sasaki T, Timpl R, Henry MD, Campbell KP. Disruption of perlecan binding and matrix assembly by post-translational or genetic disruption of dystroglycan function. FEBS Lett. 2005; 579:4792–4796. [PubMed: 16098969]
60. McDearmon EL, Combs AC, Sekiguchi K, Fujiwara H, Ervasti JM. Brain alpha-dystroglycan displays unique glycoepitopes and preferential binding to laminin-10/11. FEBS Lett. 2006; 580:3381–3385. [PubMed: 16709410]
61. Yurchenco PD, Cheng YS. Self-assembly and calcium-binding sites in laminin. A three-arm interaction model. J Biol Chem. 1993; 268:17286–17299. [PubMed: 8349613]
62. Talts JF, Sasaki T, Miosge N, Gohring W, Mann K, Mayne R, Timpl R. Structural and functional analysis of the recombinant G domain of the laminin alpha4 chain and its proteolytic processing in tissues. J Biol Chem. 2000; 275:35192–35199. [PubMed: 10934193]
63. Sztal TE, Sonntag C, Hall TE, Currie PD. Epistatic dissection of laminin-receptor interactions in dystrophic zebrafish muscle. Hum Mol Genet. 2012
64. Brockington M, Torelli S, Sharp PS, Liu K, Cirak S, Brown SC, Wells DJ, Muntoni F. Transgenic Overexpression of LARGE Induces alpha-Dystroglycan Hyperglycosylation in Skeletal and Cardiac Muscle. PLoS ONE. 2010; 5:e14434. [PubMed: 21203384]
65. Zhang P, Hu H. Differential glycosylation of {alpha}-dystroglycan and proteins other than {alpha}-dystroglycan by LARGE. Glycobiology. 2011; 22:235–247. [PubMed: 21930648]
66. Aguilan JT, Sundaram S, Nieves E, Stanley P. Mutational and functional analysis of Large in a novel CHO glycosylation mutant. Glycobiology. 2009; 19:971–986. [PubMed: 19470663]
67. Li S, Harrison D, Carbonetto S, Fassler R, Smyth N, Edgar D, Yurchenco PD. Matrix assembly, regulation, and survival functions of laminin and its receptors in embryonic stem cell differentiation. J Cell Biol. 2002; 157:1279–1290. [PubMed: 12082085]
68. Takashima Y, Era T, Nakao K, Kondo S, Kasuga M, Smith AG, Nishikawa S. Neuroepithelial cells supply an initial transient wave of MSC differentiation. Cell. 2007; 129:1377–1388. [PubMed: 17604725]
69. Foster H, Sharp PS, Athanasopoulos T, Trollet C, Graham IR, Foster K, Wells DJ, Dickson G. Codon and mRNA sequence optimization of microdystrophin transgenes improves expression and physiological outcome in dystrophic mdx mice following AAV2/8 gene transfer. Mol Ther. 2008; 16:1825–1832. [PubMed: 18766174]

70. Sharp PS, Jee H, Wells DJ. Physiological characterization of muscle strength with variable levels of dystrophin restoration in mdx mice following local antisense therapy. Mol Ther. 2011; 19:165–171. [PubMed: 20924363]

Europe PMC Funders Author Manuscripts

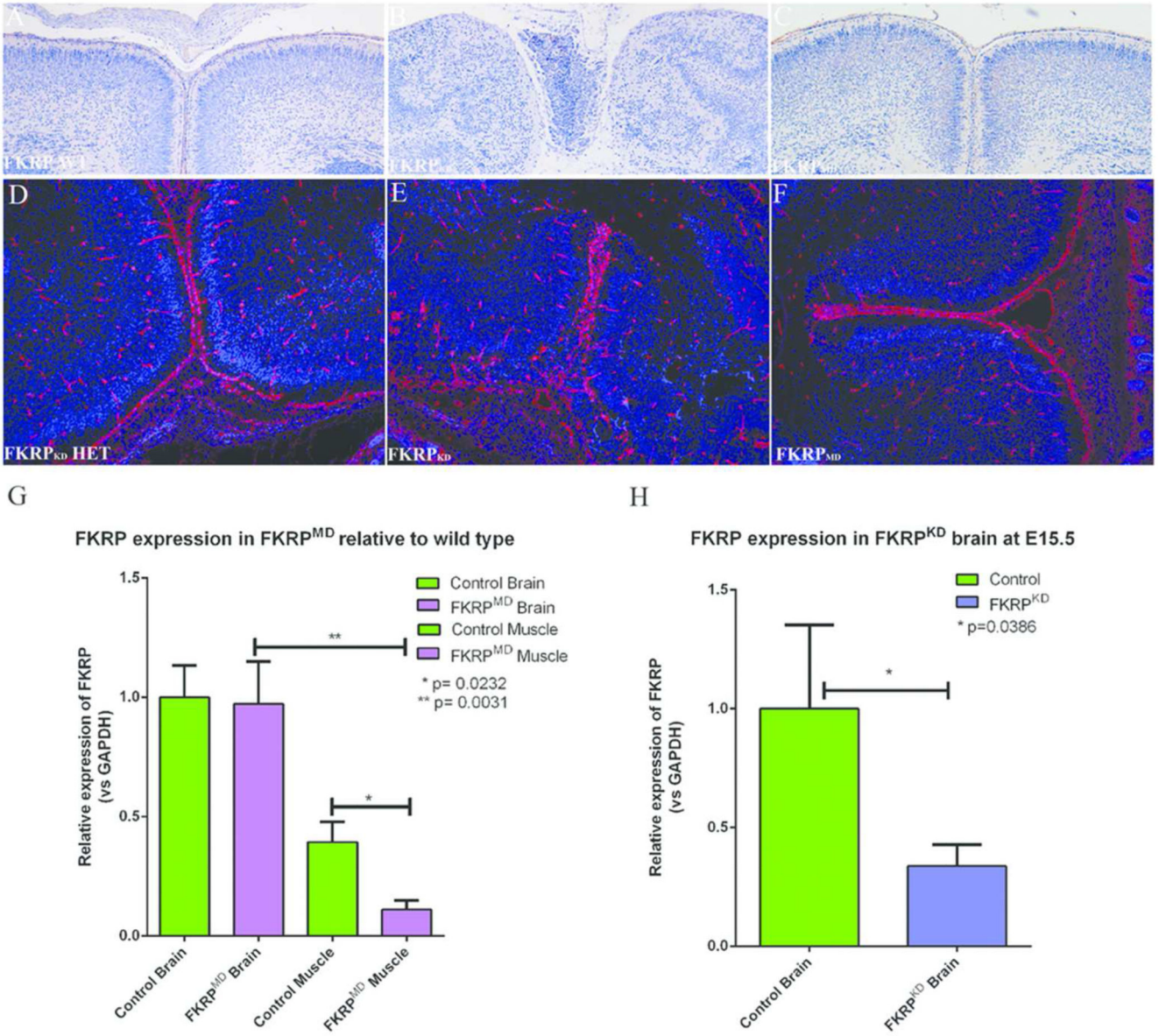

Figure 1. Real time gene expression analysis of FKRP in brain and muscle and histological evaluation of FKRP$_{MD}$ brain.

(A) IIH6 immunolabelling of haematoxylin stained coronal sections of FKRP^{KD} heterozygote (A), FKRP^{KD} (B) and FKRP$_{MD}$ (C) brains at P0. The cortical disorganisation evident in the FKRP^{KD} is no longer evident in the FKRP$_{MD}$ which now reflects that seen in the FKRP^{KD} heterozygote control. IIH6 immunolabelling can be seen at the pial basement membrane of the FKRP^{KD} heterozygote and FKRP$_{MD}$ but not the FKRP^{KD}. Immunolabelling of the pial basement membrane with a pan laminin antibody (D-F) shows the disorganisation at the intrahemispheric fissure in the FKRP^{KD}, whereas in the FKRP$_{MD}$ (F) organisation is comparable to that of heterozygote FKRP^{KD} control (D). Scale bar in images A-D are 50μm. Relative expression of FKRP (G,H). Taq man (Applied Biosystems) RT-PCR probes were used to measure relative FKRP mRNA expression in brain and skeletal

muscle of $FKRP_{MD}$ mice compared to age-matched wild type controls. Expression levels were normalised against endogenous GAPDH mRNA expression. The percentage knock-down evident in the $FKRP^{KD}$ has been maintained in the $FKRP_{MD}$ as a comparison with the levels in the $FKRP^{KD}$ brain at E15.5 show. Error bars represent SEM (n = 4). All samples were analysed as triplicate data sets. * P value = < 0.05 (two tailed t-test) ** P value < 0.005. Error bars represent ± SEM (n = 4).

Europe PMC Funders Author Manuscripts

Europe PMC Funders Author Manuscripts

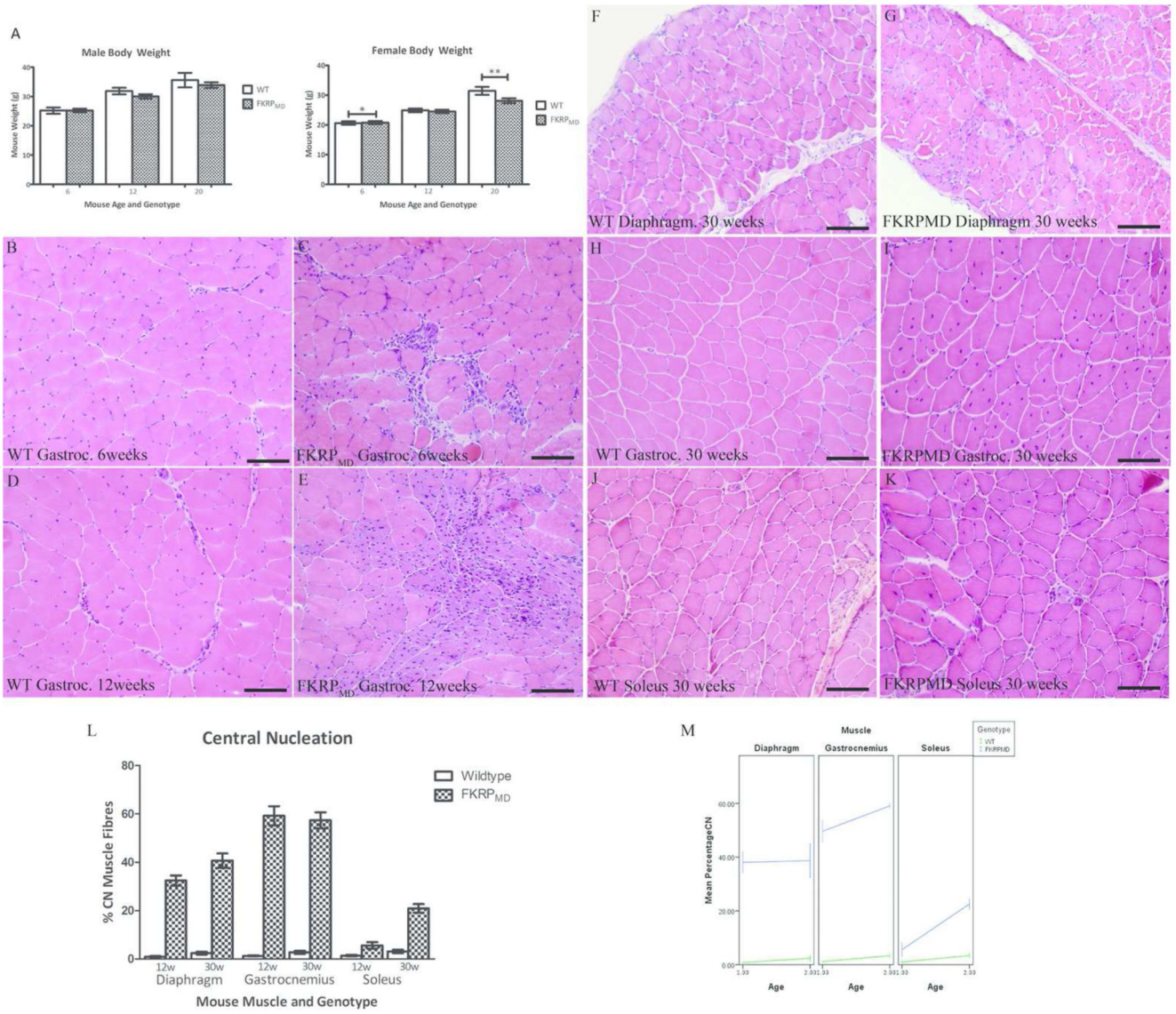

Figure 2. Body weight and histological analysis of muscle at 6, 12 and 20 weeks.

(A) Mean body weights ± SEM of male and female wildtype (white) and $FKRP_{MD}$ (patterned) at 6 weeks (male WT n=8, male $FKRP_{MD}$ n=29; female WT n=14, female $FKRP_{MD}$ n=12), 12 (male WT n=10, male $FKRP_{MD}$ n=17; female WT n=14, female $FKRP_{MD}$ n=24) and 20 weeks of age (male WT n=7, male $FKRP_{MD}$ n=13; female WT n=6, female $FKRP_{MD}$ n=12). Data were analysed with a Linear Mixed Effects Model performed using SPSS Statistics (IBM Corporation, U.S.A). This model showed that age was a significant factor affecting mouse body weight in both male and female mice, but genotype was not a significant factor affecting male body weight (p=0.245) although it was with respect to female body weight, with significance shown as follows: *0.01≤p<0.05, ** 0.001≤p<0.01. **(**B-K) Digital images of haematoxylin and eosin stained cryosections from wildtype (B,D,F,H,J) and $FKRP_{MD}$ (C,E,G,I,K) gastrocnemius (B-E, H-I) diaphragm (F-G) and quadriceps (J-K) at 6 (B-C), 12 (D-E) and 30 (F-K) weeks of age. $FKRP_{MD}$ muscle

shows evidence of inflammatory infiltrates and muscle fibre degeneration at 6 weeks of age (C), with muscle fibre regeneration seen at 12 weeks of age (D). At 30 weeks of age, centrally nucleated muscle fibres indicating previous regeneration cycles are seen in the $FKRP_{MD}$ diaphragm (G) and gastrocnemius (I). Counts of central nucleation were carried out on transverse 10μm muscle cryosections of wildtype and $FKRP_{MD}$ diaphragm, gastrocnemius and soleus at 12 and 30 weeks of age - the muscle fibres with central nuclei were counted and expressed as a percentage of the total number counted (approximately 500 for the soleus, 1500 for the diaphragm and 2000 for the gastrocnemius). The histogram in L shows the mean percentage of centrally nucleated muscle fibres ± SEM of wildtype (white) and $FKRP_{MD}$ (patterned) in the diaphragm, gastrocnemius and soleus at 12 and 30 weeks of age as indicated. This data was analysed using a General Estimating Equations Model performed using SPSS statistics which showed that age, muscle and genotype were significant factors affecting the percentage of centrally nucleated muscle fibres. The output of this model is shown as a multiple line graph in M. Scale Bars represent 50μm in B-K.

Europe PMC Funders Author Manuscripts

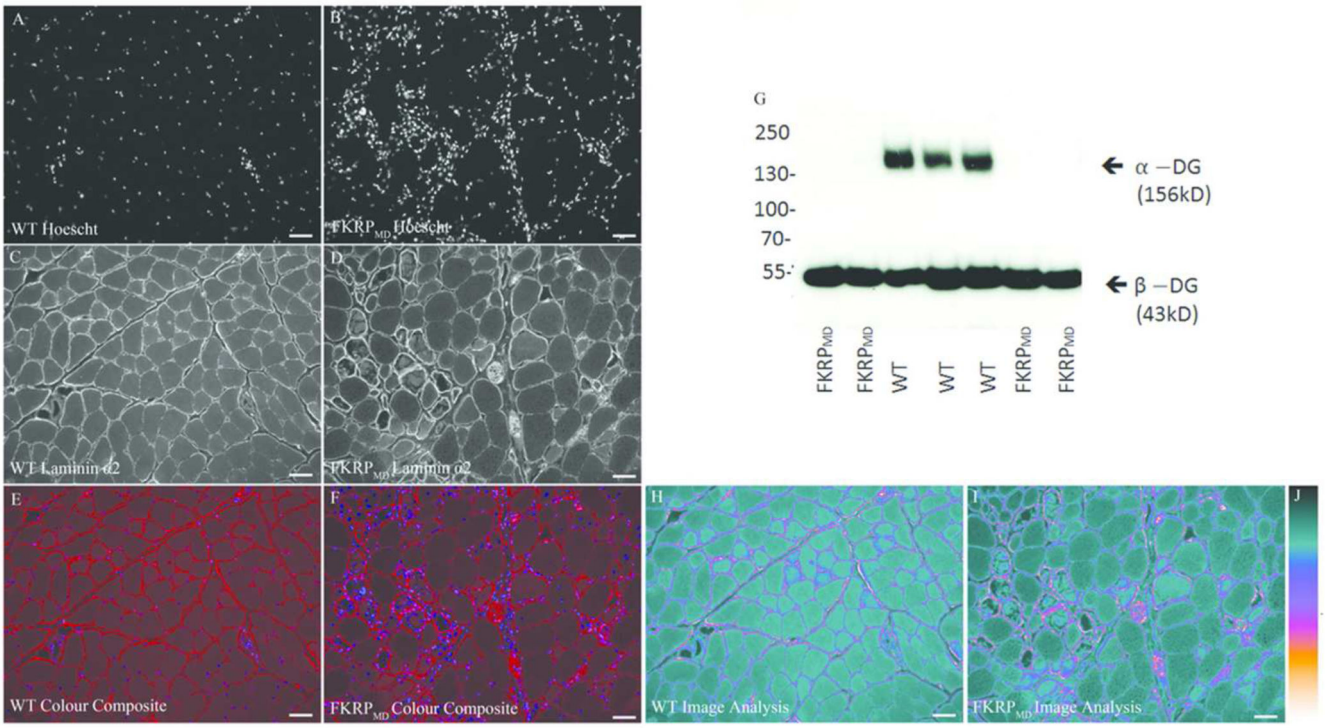

Figure 3. Immunolabelling and Western blot analysis of FKRP$_{MD}$ muscle.

Transverse 10μm cryosections from 12 week old wildtype (A,C,E) and FKRP$_{MD}$ (B,D,F) mouse triceps were labelled with Hoescht 33342 to visualise the nuclei (A-B) and an antibody against laminin α2 (C-D), with a colour composite shown in E-F. Laminin α2 immunolabelling was variable in the FKRP$_{MD}$ with small clusters of fibres showing an increase relative controls whilst the majority of other fibres displayed either similar levels to controls or a slight decrease. Scale bar represents 50μm. Western Blotting analysis (G) of quadriceps from wildtype and FKRP$_{MD}$ mice shows IIH6 labelling, present in WT mice (lanes 3,4 and 5) was absent in FKRP$_{MD}$ mice (lanes 1,2,6 and 7). Each lane contains an extract from individual animals. β-DG (43kDa) which also acts as a loading control is shown to be unchanged in the FKRP$_{MD}$. The images shown in C and D) are shown using a look up table from Image J to emphasise the variation in intensity of laminin α2 immunolabelling across the section. J shows the scale used.

Europe PMC Funders Author Manuscripts

Europe PMC Funders Author Manuscripts

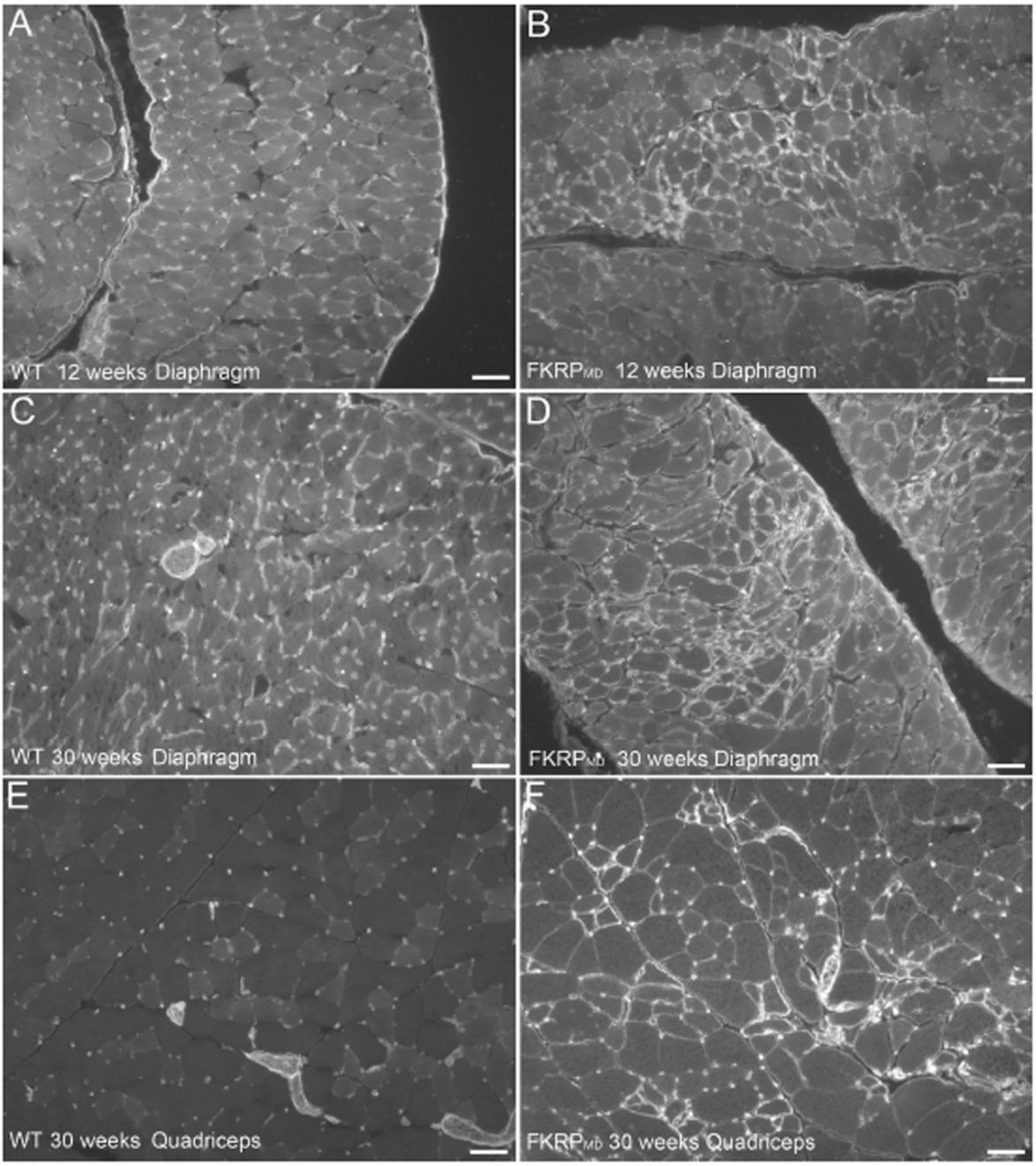

Figure 4. Laminin α4 immunolabelling of $FKRP_{MD}$ and wild type controls.

Transverse 10μm cryosections from 12 week (A-B) and 30 week (C-F) old wildtype (A,C,E) and $FKRP_{MD}$ (B, D, F) diaphragm (A-D) and rectus femoris (E,F) were immunolabelled with an antibody against laminin α4. Immunolabelling with this antibody was confined to the capillaries and nerves of wild type muscle, whereas immmunolabelling was observed at the basement membrane of small diameter fibres in the $FKRP_{MD}$ diaphragm and rectus femoris at 12 and 30 weeks of age. By 30 weeks of age laminin α4 was also evident at the basement membrane of larger diameter fibres. Scale bar represents 50μm.

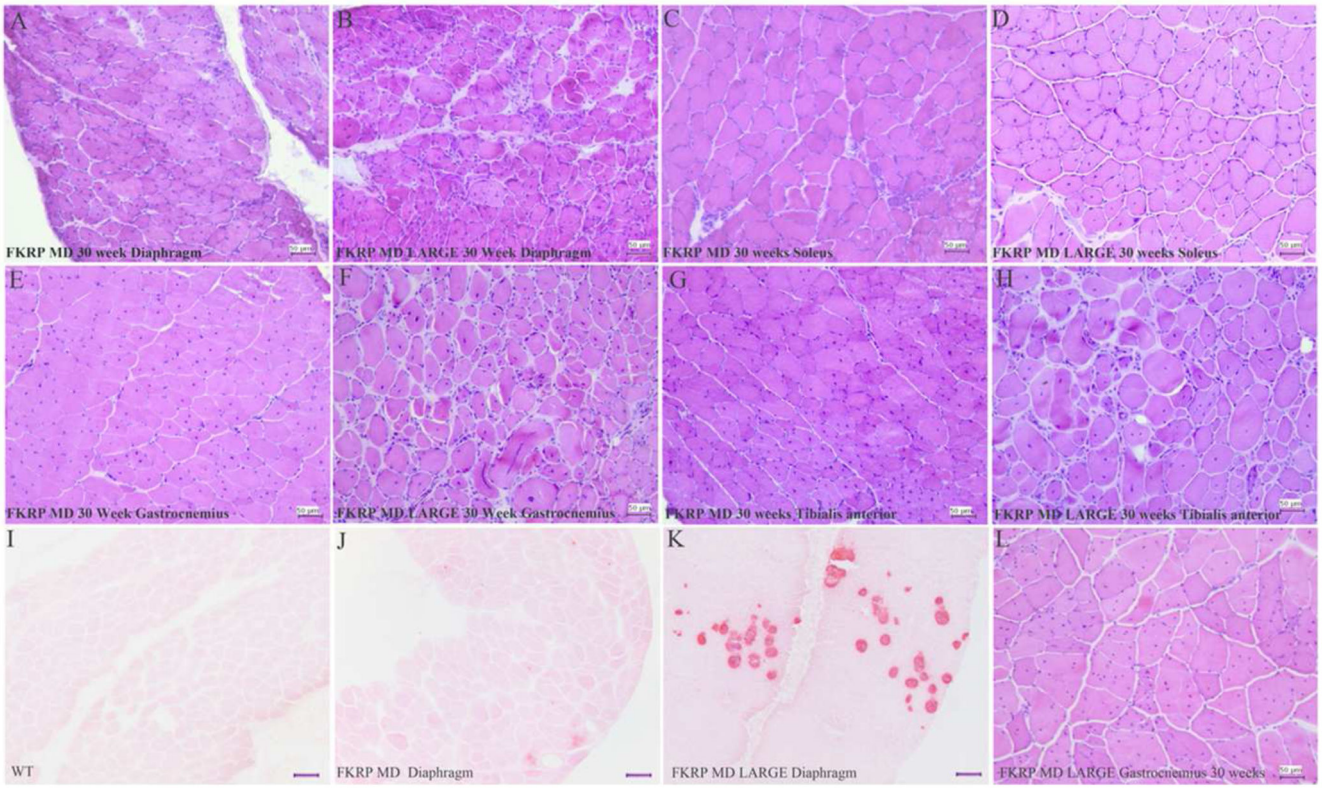

Figure 5. $FKRP_{MD}$ LARGE histology.

10μm cryosections from $FKRP_{MD}$ (A,C,E,G) and $FKRP_{MD}$LARGE (B,D,F,H) diaphragm (A-B), soleus (C-D) gastrocnemius (E-F), and tibialis anterior (G-H) at 30 weeks of age stained with haematoxylin and eosin (A-H). All muscles showed a marked variation in fibre size, the presence of degenerative fibres infiltrated with macrophages and an increase in centrally nucleated fibres relative to the $FKRP_{MD}$. I-K show Alizarin Red labelling of wildtype (I), $FKRP_{MD}$ (J) and $FKRP_{MD}$LARGE (K) diaphragm, with a greater incidence of calcium deposits (red) observed in the $FKRP_{MD}$LARGE relative to $FKRP_{MD}$. (L) is an image of a 30 week old $FKRP_{MD}$LARGE gastrocnemius, showing an example of split muscle fibres. In images A-H and L scale bar represents 50μm. In I-K scale bar represents 100μm.

Europe PMC Funders Author Manuscripts

Europe PMC Funders Author Manuscripts

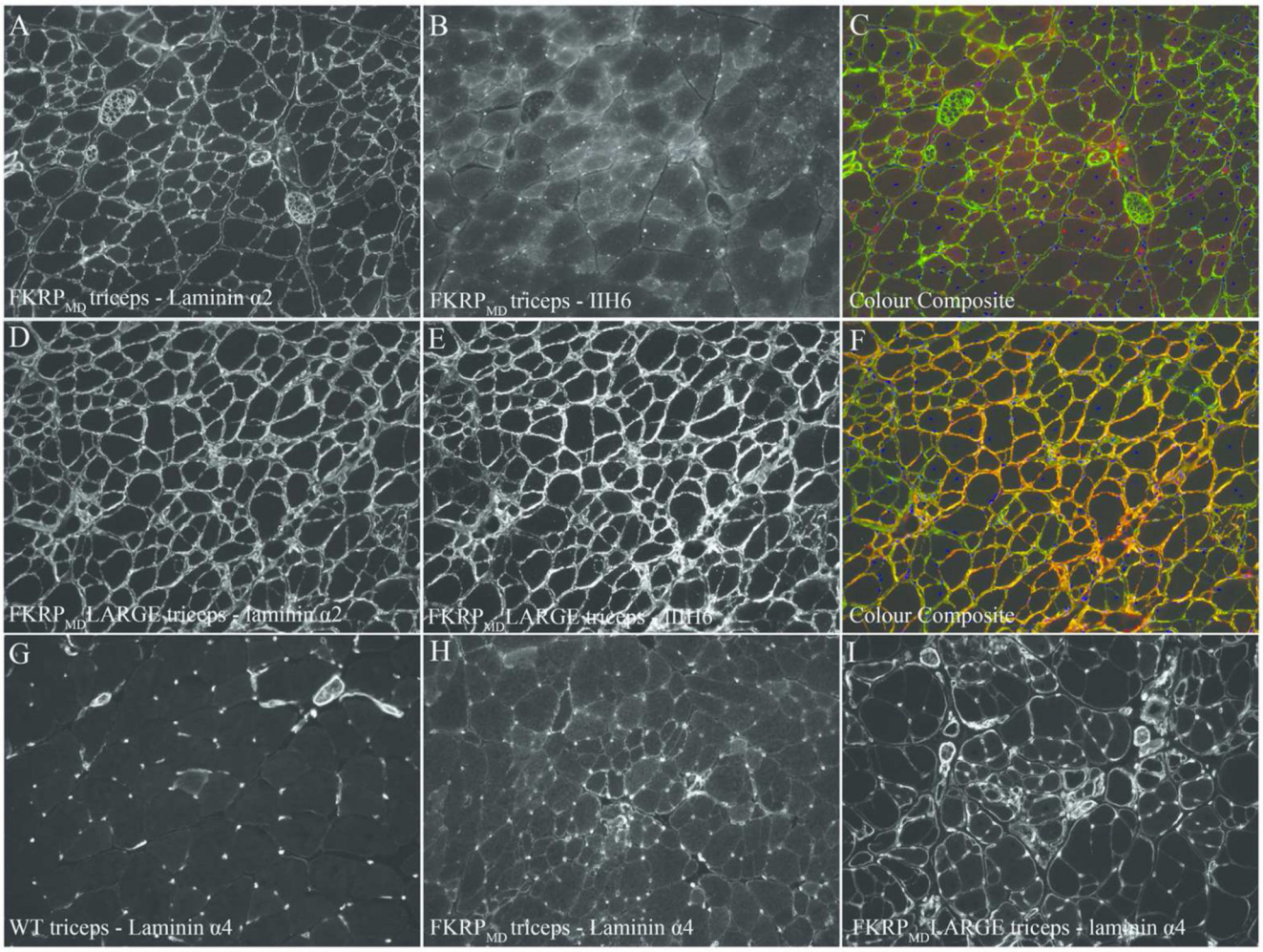

Figure 6. Immunolabelling showing a decrease in IIH6, a reduction in laminin α2 and increase in laminin α4.

Transverse 10μm cryosections of the gastrocnemius (A-D) and diaphragm (E,F) of wildtype (A,C,E) and FKRP$_{MD}$LARGE (B,D,F) mice, immunolabelled with IIH6 (antibody against glycosylated α-DG) (A,B), laminin α2 (C,D) and laminin α4 (E,F). IIH6 and laminin α2 immunolabelling was increased in the FKRP$_{MD}$LARGE mice relative to wildtype mice. Laminin α4 can be seen at the muscle fibre basement membrane of FKRP$_{MD}$LARGE mice whilst it is confined to the capillaries of wild type mice. Scale bar represents 50μm.

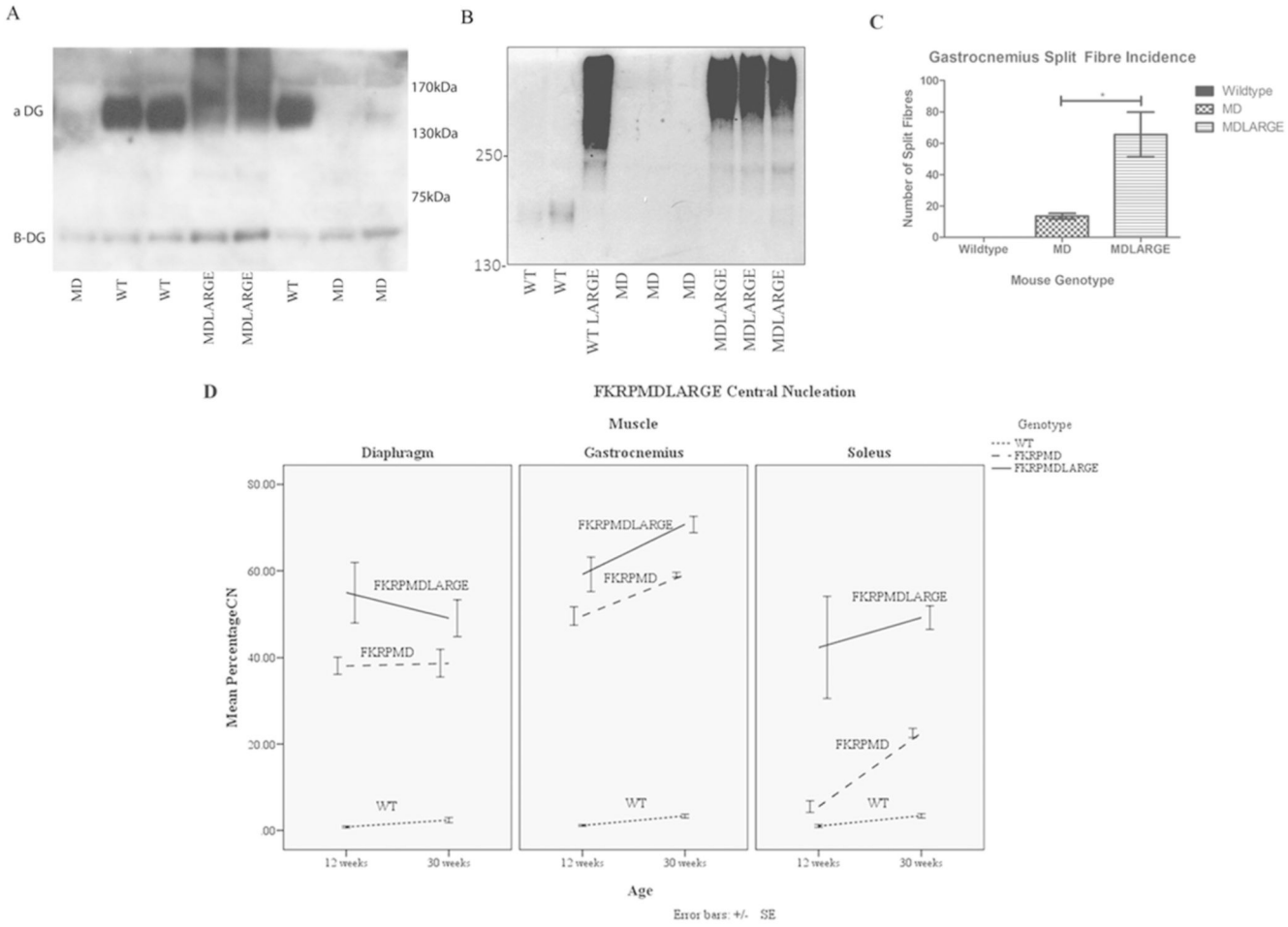

Figure 7. Ligand binding and quantitative analysis of split fibres and central nucleation.

Western blot of α and β DG of WT, $FKRP_{MD}$, $FKRP_{MD}$LARGE (A) and laminin overlay assay of wild type, wild type overexpressing LARGE, $FKRP_{MD}$ and $FKRP_{MD}$LARGE (B). As can be seen transgene expression in either the wild type or $FKRP_{MD}$ gives rise to an increase in laminin binding relative to wild type confirming that expression of the transgene led to the hyperglycosylation of α-DG. The number of split fibres in the gastrocnemius of 12 week old wildtype (n=3), $FKRP_{MD}$ (n=3) and $FKRP_{MD}$LARGE (n=3) was quantified and is shown in a histogram (C). The results of a one-tailed Mann-Whitney test are shown * $0.01 \leq p < 0.05$, illustrating a significant increase with the overexpression of LARGE on the $FKRP_{MD}$ background. (D) Counts of central nucleation were carried out on transverse 10μm cryosections of 12 and 30 week wildtype, $FKRP_{MD}$ and $FKRP_{MD}$LARGE diaphragm, gastrocnemius and soleus. Muscle fibres with central nuclei were counted and expressed as a percentage of the total number counted (approximately 500 for the soleus, 1500 for the diaphragm and 2000 for the gastrocnemius). The results of the Generalised Estimating Equations Statistical test are shown as a multiple line graph. This model shows age, muscle and genotype are significant interacting factors on the percentage of centrally nucleated muscle fibres. The $FKRP_{MD}$ data shown in Figure 2 has been included to facilitate comparisons between the $FKRP_{MD}$ and $FKRP_{MD}$LARGE models.

Europe PMC Funders Author Manuscripts

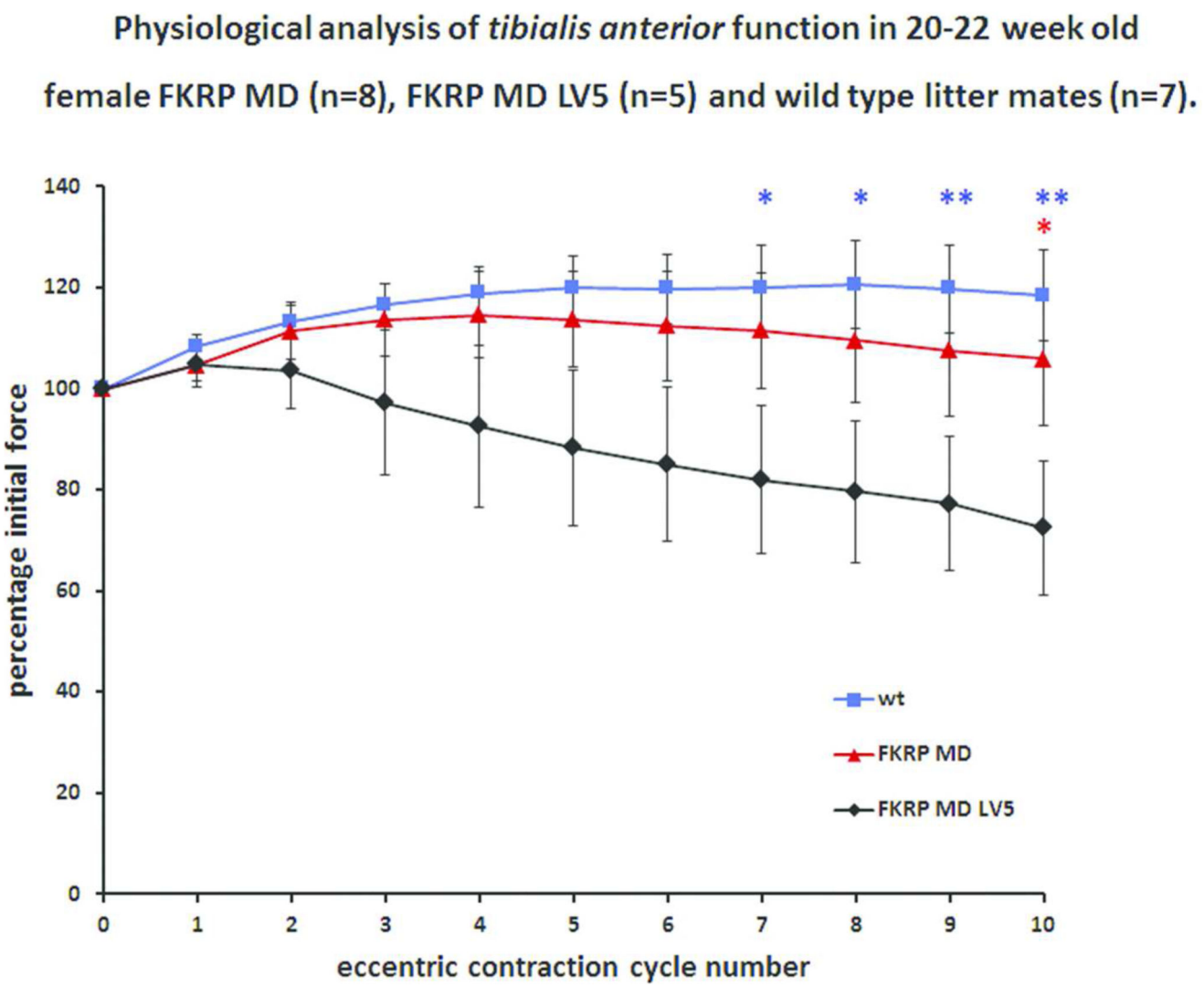

Figure 8. ***In vivo*** **assessment of muscle force production following eccentric contractions.**

Tibialis anterior muscles from 20 to 22 week old female $FKRP_{MD}$ (n=8), $FKRP_{MD}$LARGE (n=5) and wild-type (non-transgenic) mice (n=7) underwent a series of 10 eccentric contractions *in situ* utilising a stretch of 15% of optimum muscle length. The force produced by $FKRP_{MD}$ mice was not significantly different to that of wild-type animals and showed no significant drop from baseline. However, $FKRP_{MD}$LARGE mice showed a significant drop in force compared to the value at contraction 2 ($P<0.05$ for contraction 8, $P<0.01$ for contraction 9 and $P<0.001$ for contraction 10). $FKRP_{MD}$LARGE mice were significantly weaker than wild-type at contractions 7 to 10 (blue asterix symbols, * $P<0.05$, ** $P<0.01$) and weaker than $FKRP_{MD}$ mice (red asterix symbol, * $P<0.05$) after the tenth eccentric contraction. The mean force produced after 10 eccentric contractions was 118.46%, 105.83%, and 72.47 % of baseline for WT, $FKRP_{MD}$, and $FKRP_{MD}$LARGE mice respectively. Values are presented as mean and S.E.M and data are analysed using a Repeated Measures One way ANOVA with Tukey's *post-hoc* comparison.